

An Update on the Anatomy of the Forehead Compartments

Sebastian Cotofana, M.D.,
Ph.D.

Asima Mian

Jonathan M. Sykes, M.D.

Wolfgang Redka-Swoboda,
M.D.

Andrea Ladinger

Tatjana Pavicic, M.D.

Thilo L. Schenck, M.D.,
Ph.D.

Fahd Benslimane, M.D.

Fabio Ingallina, M.D.

Alexander Schlattau, M.D.

*Roseau, Commonwealth of Dominica,
West Indies; Salzburg, Austria;
Sacramento, Calif.; Munich, Germany;
Casablanca, Morocco; and Catania,
Italy*

Background: The forehead is one of the most frequent locations for neuromodulator and soft tissue filler applications; however, the underlying anatomy is still poorly understood. Thus far, the presence of deep forehead compartments has not been confirmed.

Methods: Twenty Caucasian cephalic specimens, 15 fresh frozen (six female and nine male) and five with formalin-phenol embalment (three female and two male) were investigated using contrast-enhanced computed tomographic scans, dye injections, and anatomical dissections.

Results: Three superficial (one central and two lateral) and three deep (one central and two lateral) forehead compartments were identified. The superficial fat compartments were found within the subcutaneous fat tissue (layer 2) and measured 2.1×4.6 mm for the superficial central forehead compartments and the right superficial lateral forehead compartments and 2.6×3.2 cm for the left superficial lateral forehead compartments, with a mean volume of 2.5, 3.1, and 3.4 cc, respectively. The deep fat compartments were identified deep to the frontalis muscle but superficial to the periosteum with an extent of 6.4×5.9 cm for the deep central forehead compartments, 2.6×5.8 cm for the right deep lateral forehead compartments, and 2.7×5.8 cm for the left deep lateral forehead compartments, and a mean volume of 9.1, 1.6, and 1.4 cc, respectively.

Conclusions: The results presented in this study increase the understanding of the forehead anatomy. Understanding the presence of the superficial and the deep forehead compartments allows one to change the signs of frontal aging. The deep forehead compartments are in general avascular planes and permit blunt dissection for access to the supraorbital region. (*Plast. Reconstr. Surg.* 139: 864e, 2017.)

Facial aging is a dynamic process involving all tissue layers of the face, including facial fat, facial bones, retaining ligaments of the face, muscles of facial expression, and the skin. The onset and progression of this process varies between individuals and within each individual, with each of the involved structures changing at a different pace and severity.

The forehead is one of the most frequent locations for neuromodulator and soft-tissue filler applications and is of great aesthetic interest, as it

is easily visible, located adjacent to the eyes, and often shows early signs of aging.¹ Soft-tissue fillers have been used to restore the frontal volume by injection of volumizing material into superficial and supraperiosteal locations. As every procedure should aim for the patient's safety first and natural and long-lasting results second, the understanding of the underlying anatomy is crucial for safe and effective applications on the forehead.

In 2007, Rohrich and Pessa described the presence of three distinct superficial frontal fat compartments by injecting dye into 15 fresh frozen cephalic specimen.² The authors concluded that the subcutaneous fat of the forehead is compartmentalized and that boundaries between these compartments were formed by fibrous septa, which limited the ability of the dye to migrate into other regions.

From the Department of Anatomy, Ross University School of Medicine; the Institute of Anatomy and the Department of Radiology, Paracelsus Medical University Salzburg & Nuremberg; Facial Plastic and Reconstructive Surgery, University of California Davis Medical Center; FaceSthetics, private practice, and the Department of Hand, Plastic, and Aesthetic Surgery, Ludwig-Maximilians University; Clinique Benslimane; and Clinica Di Stefano Velona.

Received for publication August 10, 2016; accepted October 18, 2016.

Copyright © 2017 by the American Society of Plastic Surgeons

DOI: 10.1097/PRS.0000000000003174

Disclosure: *The authors have no commercial associations or financial disclosures that might pose or create a conflict of interest with the results presented or methods applied in this study.*

In 2012, Gierloff and colleagues confirmed the presence of the central superficial frontal compartment (but not the two lateral superficial forehead compartments) by using computed tomographic scans and three-dimensional reconstruction when investigating nine fresh frozen cephalic specimens.^{3,4} Using this elegant technique, the authors were able to confirm the findings by Rohrich and Pessa on the forehead, but without using anatomical dissections and by thus not disrupting the delicate bounding septae. However, Gierloff et al.^{3,4} did not confirm their findings with dissections. Similarly, Rohrich and Pessa² did not correlate their findings using noninvasive procedures such as contrast-enhanced computed tomographic scanning. We therefore specifically enrolled this study using both contrast-enhanced computed tomographic scans and anatomical dissections to investigate the compartments of the forehead and to provide an update on the anatomy of this region, as current descriptions do not comprehensively explain the clinical appearance of the aging forehead.

MATERIALS AND METHODS

Study Sample

We included a total of 20 human cadaveric cephalic specimens in this study. Among those were 15 fresh frozen and five formalin-phenol embalmed specimens. While alive, all body donors gave informed consent for their bodies to be used in medical education and scientific research with medical background. All of the included body donors were of Caucasian race without any previous surgical interventions or diseases affecting the anatomical integrity of the forehead structures.

Computed Tomographic Imaging

Ten cephalic specimens were included in the computed tomographic imaging part of this investigation and originated from six female and four male cadavers, with a mean age of 72.6 ± 8.2 years. Bilateral access to the facial vein and facial artery were made to introduce an intravenous port, which was tightly secured, preventing removal. For imaging purposes, the cephalic specimens were transferred to the Department of Radiology, Paracelsus Medical University Salzburg & Nuremberg, Salzburg, Austria. Each head was placed supine and secured tightly to a head rest to maintain its position during the multiple scanning procedures. Arterial and venous contrasting was performed by injecting radiopaque dye (Iohexol Omnipaque 300, Amersham Health, Princeton, N.J.) until complete

arterial and/or venous contrasting was achieved and controlled in subsequent computed tomographic scans. Visualization of the superficial and deep compartments was accomplished by injecting Visipaque 320 mg/ml (Iodixanol; GE Healthcare, Little Chalfont, United Kingdom) in combination with Resource ThickenUp Clear (Nestle HealthCare Nutrition GmbH, Vienna, Austria). For injections into the respective forehead compartments, a 20-gauge, 70-mm sharp needle was used, with application of the material through only a single injection site. After injection of contrast agent into the respective compartments, we allowed the contrast dye to perfuse the respective compartments for a minimum of 1 hour. Multiple computed tomographic scans were obtained to ensure maximum achievable filling of the superficial and deep compartments. The following parameters were applied to each of the obtained computed tomographic scans: field of view, 200 mm; slice thickness, 0.6 mm; increment, 0.4 mm; voltage, 120 kV; and current, 400 mA/second.

Anatomical Dissection

Anatomical dissection was performed objectively on an additional five fresh frozen (all males cadavers; mean age, 71 ± 10.1 years) and five formalin-phenol embalmed (three females and two male cadavers; mean age, 77.8 ± 8.9 years) specimens at the Institute of Anatomy, Paracelsus Medical University Salzburg & Nuremberg, Salzburg, Austria; and at the Department of Anatomy, Ross University School of Medicine, Dominica, West Indies. Dissection procedures were based on a layer-by-layer identification of the forehead structures. In addition, colored dye was injected into the respective compartments to show the extent of the compartments and its bounding structures.

Data Analysis Strategy

Computed tomographic images were transferred for multiplanar image reconstruction to Philips IntelliSpace Portal (Amsterdam, The Netherlands). Three-dimensional reconstructions of the images were interpreted by the first (S.C.) and last (A.S.) authors of this study and correlated to the anatomical dissections performed by the first author (S.C.).

RESULTS

Superficial Lateral Forehead Compartments

Two superficial lateral compartments of the forehead were identified, both by computed

tomographic imaging and by dissections. According to their locations, located lateral to the superficial central forehead compartment, these compartments are termed the right and left superficial lateral frontal compartments. These compartments were identified in layer 2 (i.e., in the subcutaneous fat layer). The mean extent of the right superficial lateral frontal compartment was 2.6×3.2 cm and the mean extent of the left superficial lateral frontal compartment was 2.1×4.6 cm. The mean measured volume was 3.1 cc for the right and 3.4 cc for the left (Table 1 and Fig. 1).

The superficial boundary of the superficial lateral frontal compartment is formed by the skin (layer 1), whereas the deep boundary is formed by the frontalis muscle and its superficial fibrous fascia (layer 3). The lateral boundary is formed by the temporal ligamentous adhesions (merging point of the superior and inferior temporal septum). The inferior boundary of the superficial lateral frontal compartments is formed by the cutaneous insertion of the orbicularis oculi muscle complex (orbicularis oculi, depressor supercillii, and corrugator supercillii muscle) at the level of the eyebrow. Superiorly, the superficial lateral frontal compartments were bound by a thin fibrous septum that spanned all five layers and was identified at a mean distance of 8.8 cm laterally and 7.4 cm in the midline when measured from the superior orbital rim. We propose to term this the *superior frontal septum*, as it is located in proximity to the hairline and the coronal suture. The medial boundary of the superficial lateral frontal compartments is formed by the fibrous sheltering sheath of the supraorbital neurovascular structures that emerged at the supraorbital foramen.

Table 1. Values of the Superficial Central Forehead Compartment and the Right and Left Superficial Lateral Forehead Compartments Based on Computed Tomographic Parameters and Cadaveric Dissections

Compartment	Width (cm)	Length (cm)	Volume (cc)
SCFC			
Mean	2.1	4.6	2.5
SD	0.55	0.79	0.26
Range	1.7–2.5	3.5–4.6	2.3–2.7
SLFC right			
Mean	2.6	3.2	3.1
SD	0.13	0.95	0.14
Range	1.7–3.5	2.5–3.9	2.1–4
SLFC left			
Mean	2.1	4.6	3.4
SD	0.63	0.20	0.89
Range	1.6–2.5	4.5–4.8	2.74–4

SCFC, superficial central forehead compartment; SLFC, superficial lateral forehead compartment.

The supraorbital neurovascular structures three-dimensionally fan out after emerging from the supraorbital foramen and were identified primarily in the subcutaneous plane (layer 2) (Figs. 1 and 2). Within the compartment, small lateral frontal veins and arteries were identified that coursed primarily in a longitudinal orientation but also to a smaller portion in transverse orientation (i.e., in parallel to the eyebrow). The supraorbital vein connected with the medial zygomaticotemporal and the superficial temporal veins within this compartment (Fig. 2).

Superficial Central Forehead Compartment

The superficial central forehead compartment was identified both by computed tomographic imaging and by dissections. It was located in the subcutaneous fat and extended from the upper hairline to the root of the nose. On computed tomographic imaging, the superficial central forehead compartment was continuous with the glabella. On cadaveric dissections, however, muscle fibers of the procerus muscle inserted into the glabellar skin, and no accurate plane was identifiable during dissection of this region. Dimensions of the superficial central forehead compartment were 2.1×4.6 cm, with a mean volume of 2.51 cc (Table 1 and Fig. 1).

The superficial and deep boundaries of the superficial central forehead compartment were formed by the skin (layer 1) and the superficial fascia of the frontalis muscle (layer 3), respectively. The lateral boundaries were formed by the fibrous sheltering sheaths of the supraorbital neurovascular structures. The superior boundary was formed by the superior frontal septum, similar to that identified in the superficial lateral forehead compartment. The inferior boundary was formed by the dermal insertion of the procerus muscle emerging from the bone and inserting into the skin. Within the compartment, the constant central frontal vein and nervous branches emerging from the supratrochlear foramen were identified (Fig. 2).

Deep Lateral Forehead Compartments

The deep lateral forehead compartments were identified by both computed tomographic imaging and cadaveric dissections. The mean sizes were 2.6×5.8 cm and 2.7×5.8 cm for the right and left, respectively. The mean volumes were 1.6 cc for the right and 1.4 cc for the left deep lateral forehead compartment (Table 2 and Fig. 3). The superficial boundary of both compartments was formed by the fibrous sheet covering

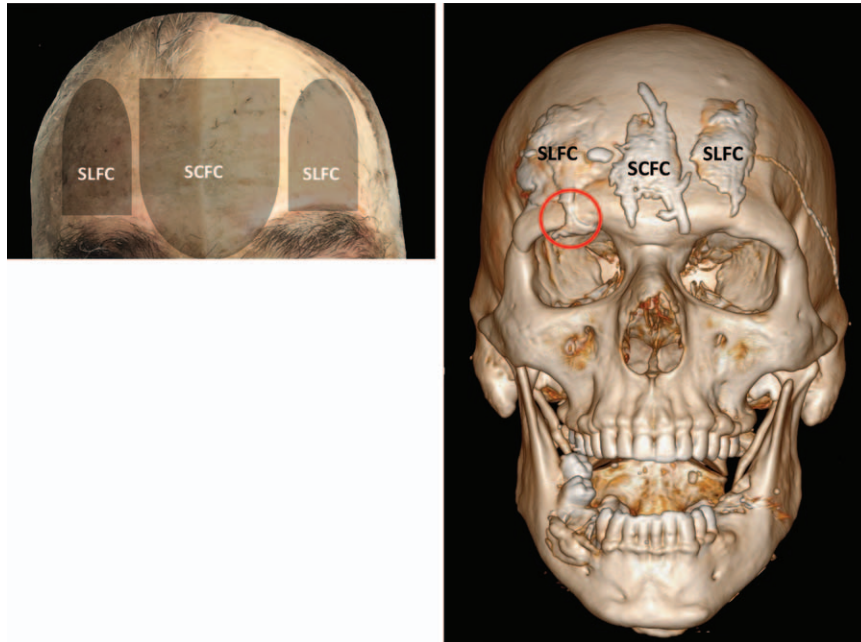


Fig. 1. Comparison between cadaveric dissection (*left*) and contrast-enhanced computed tomographic imaging (*right*). Position of the superficial forehead compartments: superficial central forehead compartment (*SCFC*) and superficial lateral forehead compartment (*SLFC*). The *red circle* shows the pathway of contrast agent retrograde to the supraorbital foramen by means of the sheath of the neurovascular bundle. Please note that because of the limited skin elasticity and the overall tissue rigidity, the extent of the superficial compartments appears smaller on imaging than in the living human.

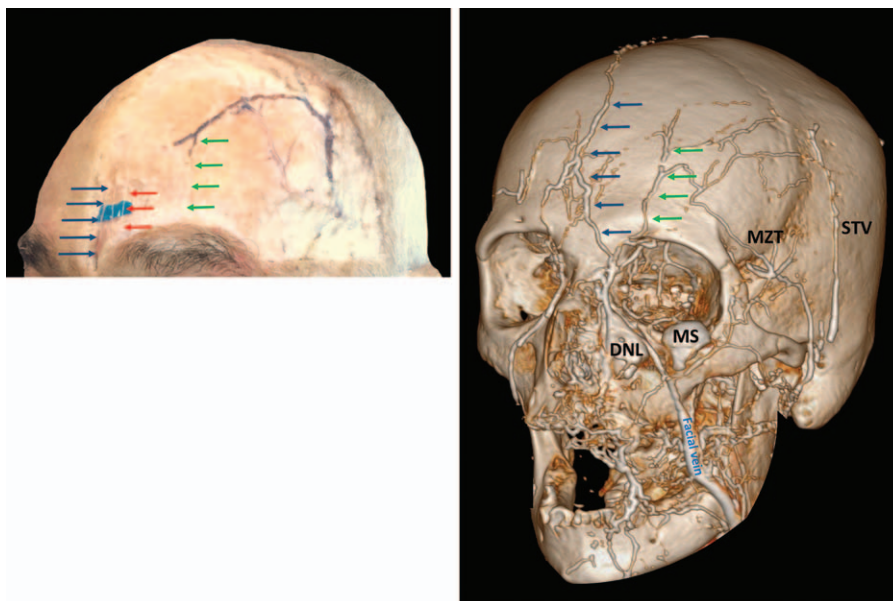


Fig. 2. Comparison between cadaveric dissection (*left*) and contrast-enhanced computed tomographic image of the facial venous system (*right*). *Blue arrows* indicate the central forehead vein, which is in connection with the angular and the supratrochlear veins, respectively. *Green arrows* indicate the supraorbital vein, which is in connection with the medial zygomaticotemporal (*MZT*) and superficial temporal vein (*STV*). The *red arrows (left)* indicate branches of the supratrochlear nerve. (*Right*) The medial part of the sub-orbicularis oculi fat (*MS*) has been contrasted, as has the deep nasolabial fat compartment (*DNL*) within the premaxillary space.

the underside of the frontalis muscle (layer 3), whereas the deep boundary was formed by the periosteum (layer 5) (Fig. 3). The lateral boundaries were formed by the temporal ligamentous adhesions. The medial boundaries were formed by the fibrous envelope of the supraorbital neurovascular structures emerging from the supraorbital foramen (Fig. 4). The inferior boundary of both deep lateral forehead compartments was formed by a septum spanning from the laterally located temporal ligamentous adhesions to the contralateral side (Fig. 5). This septum had a distance from the superior orbital rim of 1.5 ± 0.17 cm (range, 1.3 to 1.7 cm) in the midline and 3.0 ± 0.24 (range, 2.7 to 3.3 cm) at its lateral end, indicating a V-shaped orientation across the forehead, with the tip pointing inferiorly in the midline. In the following, the term *middle frontal septum* is used to name this structure. Interestingly, the location of this septum correlated well with the location of the central transverse forehead line (i.e., the deepest central forehead wrinkle when looking at the undissected forehead surface anatomy).

Deep Central Forehead Compartment

The deep central forehead compartment was identified in all of the investigated cephalic specimens, both by dissection and by computed tomographic imaging, and was located between the periosteum (layer 5) and the fascia covering the posterior surface of the frontalis muscle (layer 3) (Fig. 3). The lateral boundaries were formed by the supraorbital neurovascular structures traveling in a longitudinal orientation. The superior boundary was formed by the superior and the inferior boundary was formed by the middle

frontal septum (Fig. 5). The mean extent of the compartment was 6.4×5.9 cm, with a mean volume of 9.1 cc (Table 2 and Fig. 4). Interestingly, the applied dye filled the compartment and led to a pillow-like appearance of the compartment and was tiltable when performing subperiosteal sharp dissections (Fig. 3). No major vessels were found within this plane (layer 4).

Slightly stable longitudinal bundles of fibrous connections were identified to connect the periosteum to the underside of the frontalis muscle. These fibers were in parallel to the fiber orientation of the frontalis muscle and the supratrochlear neurovascular structures.

Additional Anatomical Observations

Superior to the lateral two-thirds of the superior orbital rim, the retro-orbicularis oculi fat compartment was identified. The retro-orbicularis oculi fat compartment was bounded inferiorly by the orbicularis retaining ligament, medially by the supraorbital neurovascular structures, and superiorly by a fibrous structure that differed from the middle frontal septum (Fig. 5). We therefore termed this septum the *inferior frontal septum* to stay consistent with the above-proposed nomenclature (Fig. 5). We also identified a thin layer of fatty tissue lying between the frontalis muscle and the fascia covering its underside. This thin fascia connected at the level of the orbital rim with the orbital septum and the orbicularis retaining ligament. Based on the results of the anatomical dissections in this study, it cannot be excluded that other compartments could be identified in future studies in relation to the corrugator supercilii, procerus, and depressor supercilii muscle.

DISCUSSION

The present study is the first combined dissection and contrast-enhanced computed tomographic imaging–based analysis investigating the superficial and the deep fat compartments of the forehead. Based on the results of this study, we were able to confirm the presence of the superficial central and the two superficial lateral forehead compartments. In addition, we were able to identify the constant presence of the deep central and the two deep lateral forehead compartments, which were located deep to the frontalis muscle but superficial to the periosteum of the frontal bone.

The strength of this investigation is the combination of noninvasive visualization techniques (i.e., contrast-enhanced computed tomographic

Table 2. Values of the Deep Central Forehead Compartment and Right and Left Deep Lateral Forehead Compartments Based on Computed Tomographic Parameters and Cadaveric Dissections

Compartment	Width (cm)	Length (cm)	Volume (cc)
DCFC			
Mean	6.4	5.9	9.1
SD	1.3	0.8	5.6
Range	4.3–7.6	4.7–6.7	5.0–19.7
DLFC right			
Mean	2.6	5.8	1.6
SD	0.47	0.21	1.50
Range	1.7–3.1	5.5–6.1	2.0–3.0
DLFC left			
Mean	2.7	5.8	1.4
SD	0.17	0.25	1.5
Range	2.5–2.9	5.3–6.0	1.0–3.0

DCFC, deep central forehead compartment; DLFC, deep lateral forehead compartment.

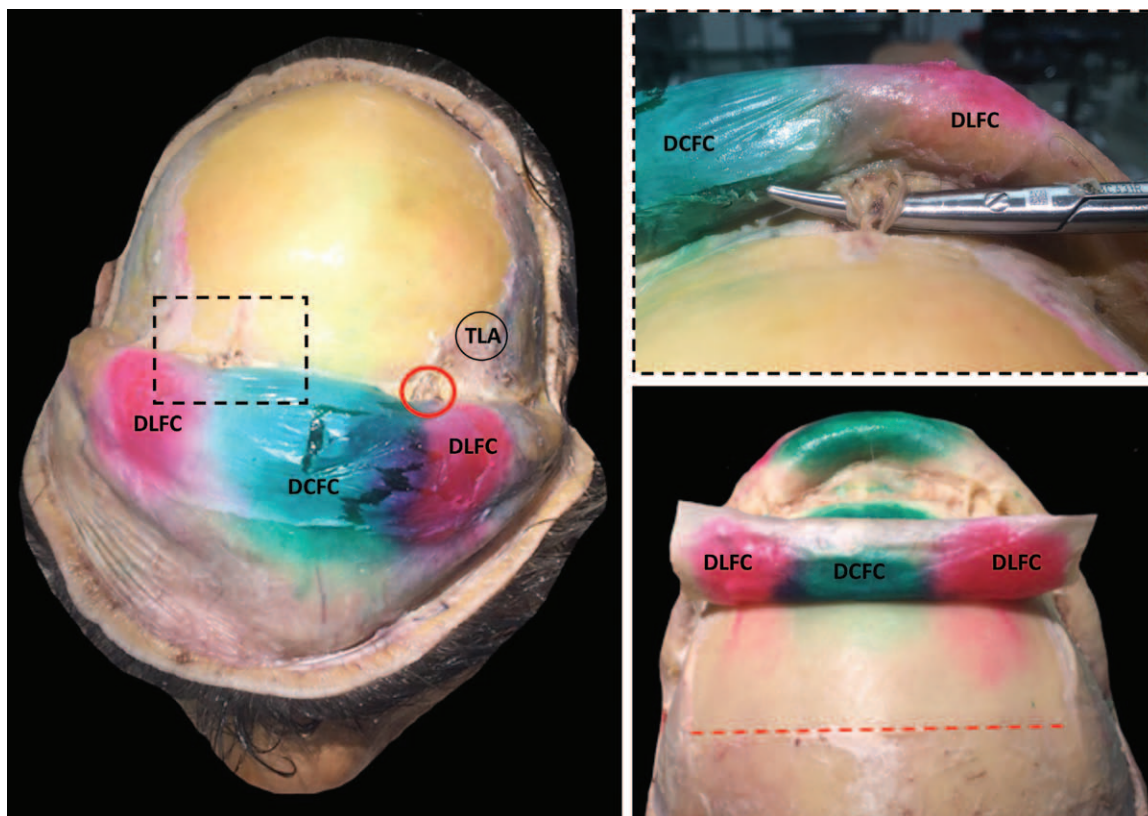


Fig. 3. Cadaveric dissection of the dye injected into the deep central forehead compartment (DCFC, green) and the deep lateral forehead compartment (DLFC, pink). Dissection was performed in the subperiosteal plane with reflection of all five layers (left). The lateral boundary of the deep lateral forehead compartment was formed by the temporal ligamentous adhesion (TLA). (Above, right) Enlargement of inset shows the supraorbital neurovascular bundle emerging from the supraorbital foramen and separating the deep central from the deep lateral forehead compartment. (Below, right) In layer 4, the deep forehead compartments were dissected and reflected. The red dotted line indicates the cut edge of the periosteum (layer 5).

imaging) that do not impair the original anatomical location of the forehead structures along with dissections performed in fresh frozen and embalmed cephalic specimens. Our results are in line with a previous study applying computed tomography–based imaging techniques, as we likewise found the presence of a superficial central forehead compartment located in layer 2 of the forehead.⁴ Our results are also in line with previous findings from anatomical dissections performed in fresh frozen specimens that used dye to contrast the superficial forehead compartments.²

However, the data presented for the measured volumes may differ from the living individual because of the applied injection technique. We specifically injected large amounts of contrast agent and dye into the respective compartments to achieve a maximum filling of each compartment and thus the best visibility possible during the imaging process. The drawback, however, of this procedure is that the applied pressure could

have permeated adjacent and/or weaker compartment boundaries and may have led to additional contrasting. Future studies might potentially find compartments that were not identified in the present work. Another limitation of this study is that we positioned the specimen in supine position in the computed tomography scanner as opposed to vertically, which would have been closer to real-life conditions.

During therapeutic applications of soft-tissue fillers into the superficial central forehead compartment, one has to be aware that by using blunt cannulas and without appropriate subcutaneous subcision procedures, the material might not migrate laterally into the superficial lateral forehead compartments and thus might not achieve a volumizing effect there. This is understandable, as the boundaries that correspond to the vertical course of the supraorbital/supratrochlear neurovasculature limit dispersal into these locations. Also, it is important to note that application of

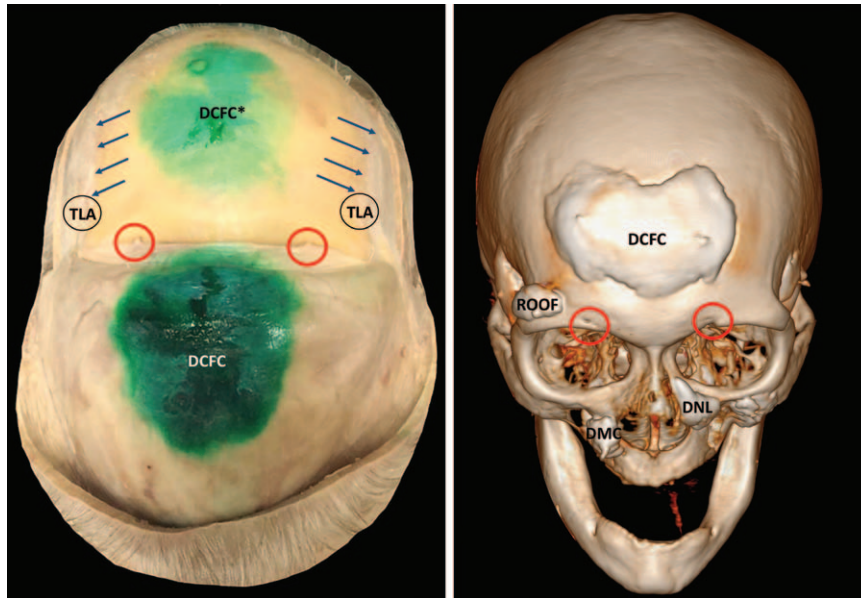


Fig. 4. Comparison between cadaveric dissection of the dye-injected deep central forehead compartment (*DCFC*) (*left*) and contrast-enhanced computed tomographic image (*right*). (*Left*) All layers of the scalp are reflected, and the underside of the periosteum is visible. The deep central forehead compartment was completely removable from the bone and its former location is indicated (*DCFC**). *Blue arrows* indicate the position of the superior temporal septum that merges with the temporal adhesion (*TLA*). *Red circles* indicate the position of the supraorbital foramen and the supraorbital neurovascular structures. (*Right*) The retro-orbicularis oculi fat (*ROOF*), the deep medial cheek (*DMC*), and the deep nasolabial (*DNL*) fat compartments (within the premaxillary space) have been contrasted also.

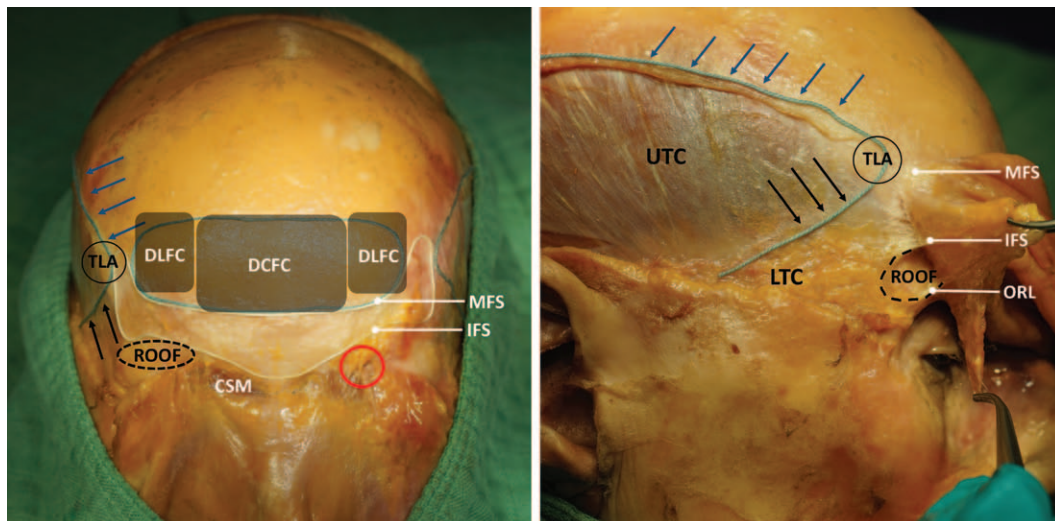


Fig. 5. Cadaveric dissection of the forehead structures on a fresh frozen specimen. Frontal (*left*) and lateral (*right*) views of the frontal and temporal regions. The frontalis muscle (layer 3) is reflected, but the periosteum (layer 5) is not detached from the bone. *TLA*, temporal ligamentous adhesion; *ROOF*, retro-orbicularis oculi fat; *CSM*, corrugator supercilii muscle; *DLFC*, deep lateral forehead compartment; *DCFC*, deep central forehead compartment; *blue arrows*, superior temporal septum; *black arrows*, inferior temporal septum; *UTC*, upper temporal compartment; *LTC*, lower temporal compartment; *red circle*, supraorbital neurovascular bundle emerging from the supraorbital foramen; *IFS*, inferior frontal septum; *MFS*, middle frontal septum; *ORL*, orbicularis retaining ligament.

material into the superficial central compartment in proximity to the superior orbital rim might gain access to the upper lid through the canal that is formed by the neurovascular structures and could thus affect the appearance and function of the upper lid (Fig. 1).

To the best knowledge of the authors, this is the first investigation to demonstrate the presence of three forehead compartments deep to the frontalis muscle but superficial to the periosteum of the frontal bone (Fig. 3). During application of contrast agent into the deep central forehead compartment, a consistent vertical spread of the contrast agent was observed without major lateral distribution to the injection site. This phenomenon can also be observed clinically when applying volume-enhancing materials with keeping the needle or cannula in constant contact with the bone during the entire procedure. The anatomical correlate for this phenomenon is represented by short but weak longitudinal fibrous adhesions extending from the fascia covering the posterior side of the frontalis muscle to the periosteum

potentially related to the course of the supratrochlear neurovascular structures. These irregularities can persist even after mechanical manipulation and are more prominent when using material with high viscoelastic properties. Distribution of the material (i.e., by using a blunt cannula) during the application and by thus breaking through the septa can lead to a smooth dispersal and a satisfying result (Fig. 6).

A previous study by Moss et al.⁵ described the ligamentous structures of the forehead and reported a 20- to 40-mm-long ligamentous adhesion in the lateral forehead, a temporal ligamentous adhesion and a fibrous adhesion spanning the entire forehead and connecting both the temporal ligamentous adhesions from each side, and a supraorbital ligamentous adhesion.^{5,6} Our results confirm the presence of this structure, as it forms the inferior boundary of the deep lateral frontal compartments. We could also confirm the presence of the supraorbital ligamentous adhesion, as this structure forms the inferior boundary of the deep central forehead compartment.

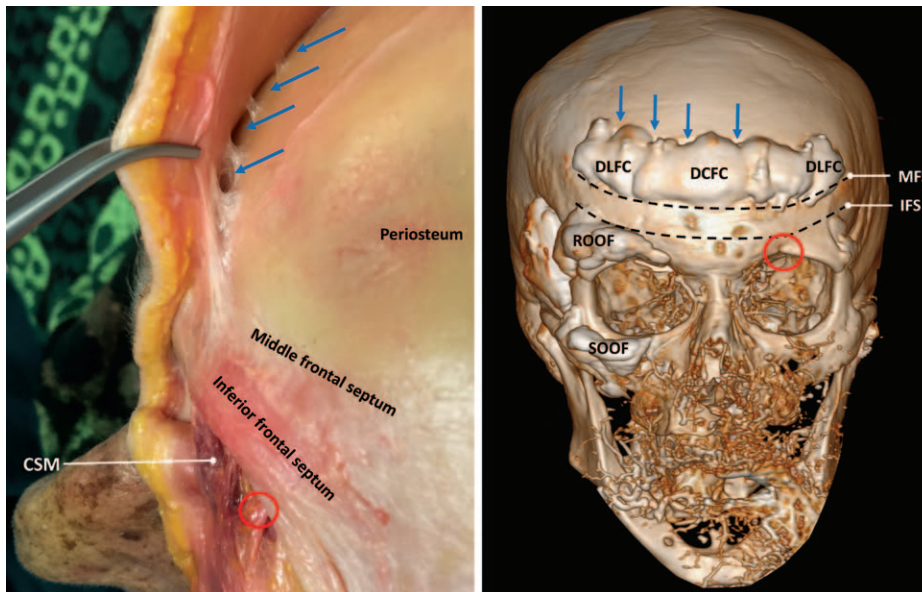


Fig. 6. Comparison between cadaveric dissection (*left*) and contrast-enhanced computed tomographic imaging (*right*) of the three deep forehead compartments: left and right deep lateral forehead compartments (DLFC) and deep central forehead compartment (DCFC). (*Left*) Cadaveric dissection shows the short longitudinal fibrous bands connecting the periosteum to the fascia covering the underside of the frontalis muscle in the view from superolateral onto layer 4. CSM, corrugator supercillii muscle; red circle, supraorbital neurovascular bundle. (*Right*) Contrast-enhanced computed tomographic scan shows the results of the application of contrast agent into all three deep compartments of the forehead (left and right deep lateral forehead compartments and deep central forehead compartment) by using a blunt cannula and distributing the material throughout the forehead and by thus rupturing the boundaries of the respective compartments. IFS, inferior frontal septum; MFS, middle frontal septum; SOOF, sub-orbicularis oculi fat; ROOF, retro-orbicularis oculi fat.

Because of the nature of these structures, we propose the names *middle frontal septum* and *inferior frontal septum*, as these structures bound compartments and limit the migration of applied materials of the forehead. Interestingly, we found several additional fat compartments between these two septae that were in relation to the corrugator supercillii muscle and the retro-orbicularis oculi fat; however, further anatomical studies will be needed to confirm their constant presence and their precise location within the different layers of the forehead.

During the process of aging, it has been shown that the orbital region undergoes changes with regard to bone remodeling.^{7,8} Likewise, it has been shown that the shape of the forehead (when viewed laterally) loses its convexity and gains a concave shape resembling the process of frontal hollowing. Volume-enhancing strategies should aim for a longer lasting and profound volumizing and lifting effect. Using the deep forehead compartments, volumizing materials can be placed in these locations, and manual modulation can be used to distribute the applied volume for restoration of the convexity of the forehead.^{9–12} The applied material can be molded throughout the extent of the respective compartment without serious risk of injury because this plane (i.e., layer 4) is generally avascular and without the presence of major neurovascular structures within the compartments (but not within the boundaries of the compartments).

CONCLUSIONS

The understanding of the presence of superficial and deep forehead compartments allows one to change the signs of aging of the forehead. Three superficial (one central and two lateral) and three deep (one central and two lateral) forehead compartments were identified, combining contrast-enhanced computed tomographic imaging with anatomical dissections. The results presented in this study increase the understanding of the forehead anatomy relevant for volumizing procedures. Future studies applying different invasive and noninvasive methods will be needed to confirm the findings presented and to provide continuative insights on the additional anatomical observations found in this study.

Sebastian Cotofana, M.D., Ph.D.

Department of Anatomy
Ross University School of Medicine
P.O. Box 266

Roseau, Commonwealth of Dominica, West Indies
sebastiancotofana@rossu.edu

ACKNOWLEDGMENTS

The imaging part of this study was funded by Merz Pharmaceuticals GmbH (grant number 13072015). The authors would like to thank Mathias Hessenberger, Markus Schlager, and Ashley Nicole Davis for tremendous support in the anatomical and imaging parts of this study.

REFERENCES

1. American Society of Plastic Surgeons. 2015 cosmetic plastic surgery statistics. Available at: <https://d2wirczt3b6wjw.cloudfront.net/News/Statistics/2015/plastic-surgery-statistics-full-report-2015.pdf>. Accessed August 15, 2016.
2. Rohrich RJ, Pessa JE. The fat compartments of the face: Anatomy and clinical implications for cosmetic surgery. *Plast Reconstr Surg*. 2007;119:2219–2227; discussion 2228–2231.
3. Gierloff M, Stöhring C, Buder T, Gassling V, Açil Y, Wiltfang J. Aging changes of the midfacial fat compartments: A computed tomographic study. *Plast Reconstr Surg*. 2012;129:263–273.
4. Gierloff M, Stöhring C, Buder T, Wiltfang J. The subcutaneous fat compartments in relation to aesthetically important facial folds and rhytides. *J Plast Reconstr Aesthet Surg*. 2012;65:1292–1297.
5. Moss CJ, Mendelson BC, Taylor GI. Surgical anatomy of the ligamentous attachments in the temple and periorbital regions. *Plast Reconstr Surg*. 2000;105:1475–1490; discussion 1491.
6. O'Brien JX, Ashton MW, Rozen WM, Ross R, Mendelson BC. New perspectives on the surgical anatomy and nomenclature of the temporal region: Literature review and dissection study. *Plast Reconstr Surg*. 2013;132:461e–463e.
7. Pessa JE, Desvigne LD, Lambros VS, Nimerick J, Sugunan B, Zadoo VP. Changes in ocular globe-to-orbital rim position with age: Implications for aesthetic blepharoplasty of the lower eyelids. *Aesthetic Plast Surg*. 1999;23:337–342.
8. Cotofana S, Fratila A, Schenck TL, Redka-Swoboda W, Zilinsky I, Pavicic T. The anatomy of the aging face: A review. *Facial Plast Surg*. 2016;32:253–260.
9. Wulc AE, Sharma P, Czyz CN. The anatomic basis of midfacial aging. In: Hartstein EM, Wul EA, Holck EED, eds. *Midfacial Rejuvenation*. New York: Springer; 2012:15–28.
10. Bartlett SP, Grossman R, Whitaker LA. Age-related changes of the craniofacial skeleton: An anthropometric and histologic analysis. *Plast Reconstr Surg*. 1992;90:592–600.
11. Farkas JP, Pessa JE, Hubbard B, Rohrich JR. The science and theory behind facial aging. *Plast Reconstr Surg Global Open* 2013;1:e8–e15.
12. Carruthers J, Carruthers A. Volumizing the glabella and forehead. *Dermatol Surg*. 2010;36(Suppl 3):1905–1909.